JOINT EUROPEAN TORUS

JET–P(92)79

F. Tibone, B. Balet, M. Bures, J.G. Cordey, T.T.C. Jones, P.J. Lomas, K. Lawson,
H.W. Morsi, P. Nielsen, D.F. Start, A. Tanga, A. Taroni, K. Thomsen,
D.J. Ward and JET Team

Dependence of Confinemet on Plasma Ion Species in JET

Dependence of Confinemet on Plasma Ion Species in JET

F. Tibone, B. Balet, M. Bures, J.G. Cordey, T.T.C. Jones, P.J. Lomas, K. Lawson, H.W. Morsi, P. Nielsen, D.F. Start, A. Tanga, A. Taroni, K. Thomsen, D.J. Ward and JET Team*

JET-Joint Undertaking, Culham Science Centre, OX14 3DB, Abingdon, UK

** See Annex*

Preprint of Paper to be submitted for publication in
Nuclear Fusion Letters

DEPENDENCE OF CONFINEMENT ON PLASMA ION SPECIES IN JET

F Tibone, B Balet, M Bures, JG Cordey, TTC Jones, PJ Lomas, K Lawson, HW Morsi, P Nielsen, DF Start, A Tanga, A Taroni, K Thomsen, DJ Ward

JET Joint Undertaking, Abingdon Oxon OX14 3EA, U.K.

ABSTRACT

The properties of JET plasmas obtained in similar conditions, but using different ion species, are compared. In hydrogenic limiter discharges with NBI heating, particle confinement and sawtooth activity display a strong isotopic dependence. However, the improvement in global energy confinement from hydrogen to deuterium is only approximately 20%, not consistent with the square-root dependence $\tau_E \sim A_i^{1/2}$ often found in L-mode scaling relationships. No significant change in energy or particle confinement is observed when deuterium is replaced by helium-3.

INTRODUCTION

Many empirical scaling relationships for energy confinement in tokamaks (e.g. [1]) include a dependence of the energy replacement time $\tau_E \sim A_i^{\alpha}$ with $\alpha \approx 1/2$, A_i being the atomic mass of the plasma ion species. However, no convincing theoretical justification has so far been found for such a dependence; classical transport would lead us to expect $\alpha = -1/2$, and so would some theories of anomalous transport (e.g. those based on drift wave turbulence).

To study the problem in JET, a series of well diagnosed discharges has been performed with different gas species, namely hydrogen (H), deuterium (D)

and the helium isotope ^{3}He. Care has been taken to avoid mixture of different ions and to obtain discharges with the same plasma configuration, current, toroidal magnetic field, and similar density and power deposition profiles. These aims have been achieved in discharges with neutral beam injection (NBI). The main limitation has been the maximum NBI power with hydrogen beams which could not exceed 7MW. This limitation has not allowed an extension of the study to comparisons of hydrogen and deuterium H-modes, as the available power was not enough to achieve good H-modes in hydrogen. However, a complete set of reference discharges has been obtained for H, D and ^{3}He L-mode discharges in the limiter configuration. The main plasma parameters are I = 3.1MA, B = 2.9T, $P_{NBI} \approx 6$MW with volume averaged electron density in the range $\langle n_e \rangle \simeq 1.5 - 3.5 \times 10^{19} m^{-3}$. D and ^{3}He reference shots at $P_{NBI} \approx 12$MW and densities up to $4.5 \times 10^{19} m^{-3}$ have also been obtained.

DEPENDENCE ON HYDROGENIC ISOTOPE

We first compare data from an L-mode density scan in hydrogen plasmas (with hydrogen neutral beam injection) with those from similar limiter discharges in deuterium. The additional heating power is $P_{NBI} = 6.0 \pm 0.5$ MW. In the hydrogen discharges the residual deuterium concentration, as measured by the neutral particle analyzer, is less than 10% (which is consistent with the measured D-D neutron yield).

The time evolution of two discharges, one in D and one in H, with similar density and input power is shown in Figure 1. The (sawtooth-averaged) profiles measured in steady state using interferometry and electron cyclotron emission are compared in Figure 2. The central T_e signal in Figure 1 shows that sawteeth are approximately twice as frequent in H as in D. The total energy content measured by the diamagnetic loops is 15-20 % larger in deuterium. This is reflected in a higher electron temperature, for the same plasma density.

In hydrogen only the central ion temperature has been measured, and $T_{io} \simeq T_{eo}$ at all densities. Profile measurements in the deuterium discharges show $T_i \simeq T_e$ to within 10% at all radii; study of the local power balance for the two fluids separately then indicates that the heat loss via the ion channel is at least as important as that via the electron channel. Throughout the analysis that follows, it has been assumed that $T_i(r) \simeq T_e(r)$ also for the hydrogen plasmas - which has similar implications for the relative heat flows. Impurity content, Ohmic and radiated power are similar for both isotopes at all densities.

The NBI injection energy was lower in hydrogen than in deuterium (approximately 100 keV compared with approximately 140 keV). In addition, the different neutralization efficiencies meant that more of the H^o beam power was delivered at reduced energy (the splitting into full/half/third energy components due to molecular effects in generating the beams is approximately 40/30/30 in hydrogen as opposed to 65/20/15 in deuterium). As a result, the particle source was stronger in hydrogen, while the energy stored in the fast ion population was larger in deuterium (which may account for the difference in sawtooth behaviour). The power deposition profiles, however, are very similar both in their radial distribution and in the ratio of ion to electron heating. These results are summarized in Figure 3, based on calculations with the PENCIL code that have been confirmed in selected cases by TRANSP.

The energy replacement time has been evaluated using the measured plasma profiles and the NBI modelling referred to above, and is shown in Figure 4, where each data point corresponds to one discharge in approximate steady-state conditions. The thermal energy confinement is higher in deuterium, with $[\tau_E(D) - \tau_E(H)]/\tau_E(D) = (15 \pm 8)\%$. We regard the systematic difference as statistically significant, even though the addition of absolute "error bars" on individual data points (typically $\pm$ 15%) could lead to an overlap of H and D data. This is because the same diagnostic measurements and identical analysis techniques were used in all cases. Inclusion of the fast ion energy enhances the

difference between τ_E in H and D, which in average however does not exceed 25%.

The difference between H and D is more marked if one looks at particle confinement. This appears to be significantly worse in hydrogen, since similar density profiles are sustained in spite of a stronger beam fuelling. Figure 5 shows the particle confinement time $\tau_p \equiv \int n_e dV/\Gamma_e$ of electrons within $r/a = 0.7$, where Γ_e is the local electron flux, for a radial position well outside the region affected by sawteeth.

The global confinement properties are reflected in Figures 6 and 7 in terms of "effective" local transport coefficients, evaluated outside the sawtooth region. Figure 6 shows an electron diffusion coefficient defined as $D_{eff} = - \Gamma_e/\nabla n_e$, which exhibits a clear isotopic dependence. (We cannot, of course, exclude the possibility that the difference in particle confinement is due to a change in a pinch term in the particle flux, with the actual diffusion unaffected). Note that at $r/a = 0.7$ the particle flux is due mostly to the neutral beam source, with a negligible contribution from edge recycling.

Figure 7 shows the variation of a local one-fluid thermal conductivity, defined as $\chi_{eff} = - (q_e + q_i)_{COND}/(n_e \nabla T_e + n_i \nabla T_i)$, at two radial locations in the plasma as a function of the input power per particle; the total heat flux has been split as $q_{TOTAL} = q_{COND} + \lambda \Gamma T$. χ_{eff} may be marginally lower in deuterium than in hydrogen (no difference is seen in fact if $\lambda = 5/2$), but clearly this does not explain the entire difference in global energy confinement. Part of this difference is due to the fact that, as a result of the lower particle confinement, the convective heat flux $\lambda \Gamma T$ in hydrogen is larger than in deuterium. Even if this term accounts for only 10-20% of the net heat flux, the effect contributes to the global difference. A further contribution of approximately 5% is due to the more frequent sawteeth in hydrogen.

COMPARISON BETWEEN DEUTERIUM AND HELIUM-3 DATA

Injection of ^{3}He neutral beams into ^{3}He plasmas has been performed up to an input power of 12 MW; the main parameters are compared with those of a similar deuterium discharge in Figure 8. The effort to keep all plasma parameters unchanged, when replacing D with ^{3}He, was less successful than in the isotope exchange experiment discussed above. The helium plasmas have higher density, lower impurity content and lower radiative losses compared to the equivalent deuterium discharges. The plasma volume was also 10% larger in the case of ^{3}He.

Figure 9 shows that there is little difference in the estimated thermal energy replacement time between the two ion species. NBI modelling indicates that W_{fast} is again larger in deuterium, and that ^{3}He injection leads to more electron than ion heating. The effective one-fluid thermal conductivity is systematically larger by ~ 20 % in the outer plasma in the case of helium, as shown in Figure 10. This increase in transport offsets the favourable effect on the global confinement of larger volume and lower power losses by radiation in ^{3}He. No evidence has been found for a significant difference in particle confinement between D and ^{3}He.

DISCUSSION OF RESULTS

We have presented results of the first experiments in JET explicitly designed and carried out to investigate in a controlled way the effects of a change in the plasma ion species used. They show that energy confinement in the L-mode regime is only weakly dependent on the ion mass.

In the hydrogenic plasmas, particle confinement and sawtooth activity are observed to respond sensitively to the exchange of isotope; in this respect, JET plasmas behave similarly to those of ASDEX [2,3]. The different sawtooth behaviour is correlated with a difference in energetic ion population due to the change in NBI parameters.

The observation that $\tau_{p,el}$ increases by ~ 50% from hydrogen to deuterium remains unexplained, but it does indicate that a change in ion species can affect the local particle transport. Global energy confinement, on the other hand, is less sensitive, increasing only by about 20% when deuterium replaces hydrogen.

This indicates that L-mode scaling relationships which suggest $\tau_E \sim A_i^{1/2}$ (as for example the ITER89P scaling [1]) is not a good description of JET plasmas. The isotope dependence of τ_E in JET is weaker than that reported in ASDEX [3], but appears to be consistent with observations in larger tokamaks, such as DIII-D [4] and TFTR [5].

We interpret the observed difference in τ_E between hydrogen and deuterium plasmas as being due to several small factors: the effect of particle confinement and sawteeth on the energy balance, the reduced fast ion population in hydrogen and possibly a modest decrease in conductive heat transport in deuterium.

No improvement in thermal energy or particle confinement is observed in JET L-modes when deuterium is replaced by helium - 3. On the contrary, local analysis of the ^{3}He data shows a slight degradation in the conductive transport near the plasma edge.

References

[1] Yushmanov P.N., Takizuka T., Riedel K.S.., et al., *Nucl. Fusion* **30**(1990)1999.

[2] Gehre O., Gentle K.W., and the ASDEX Team, *Europhys. Conf. Abstr.* **15C**(Proc. 18th EPS Conference, Berlin 1991)Vol. I, p97.

[3] Wagner F., Bessenrodt-Weberpals M., Giannone L., et al., *Europhys. Conf. Abstr.* **14B**(Prof. 17th EPS Conference, Amsterdam 1990) Vol. I, p58.

[4] Schissel D.P., et al., *Nucl. Fusion* **29**(1989)185.

[5] Grisham L. and the TFTR Group, "Thermal Confinement in TFTR L-Modes and Supershots", presented at the Large Tokamak Cooperation Workshop W22, JAERI, Naka, Japan, 18-20 May 1992.

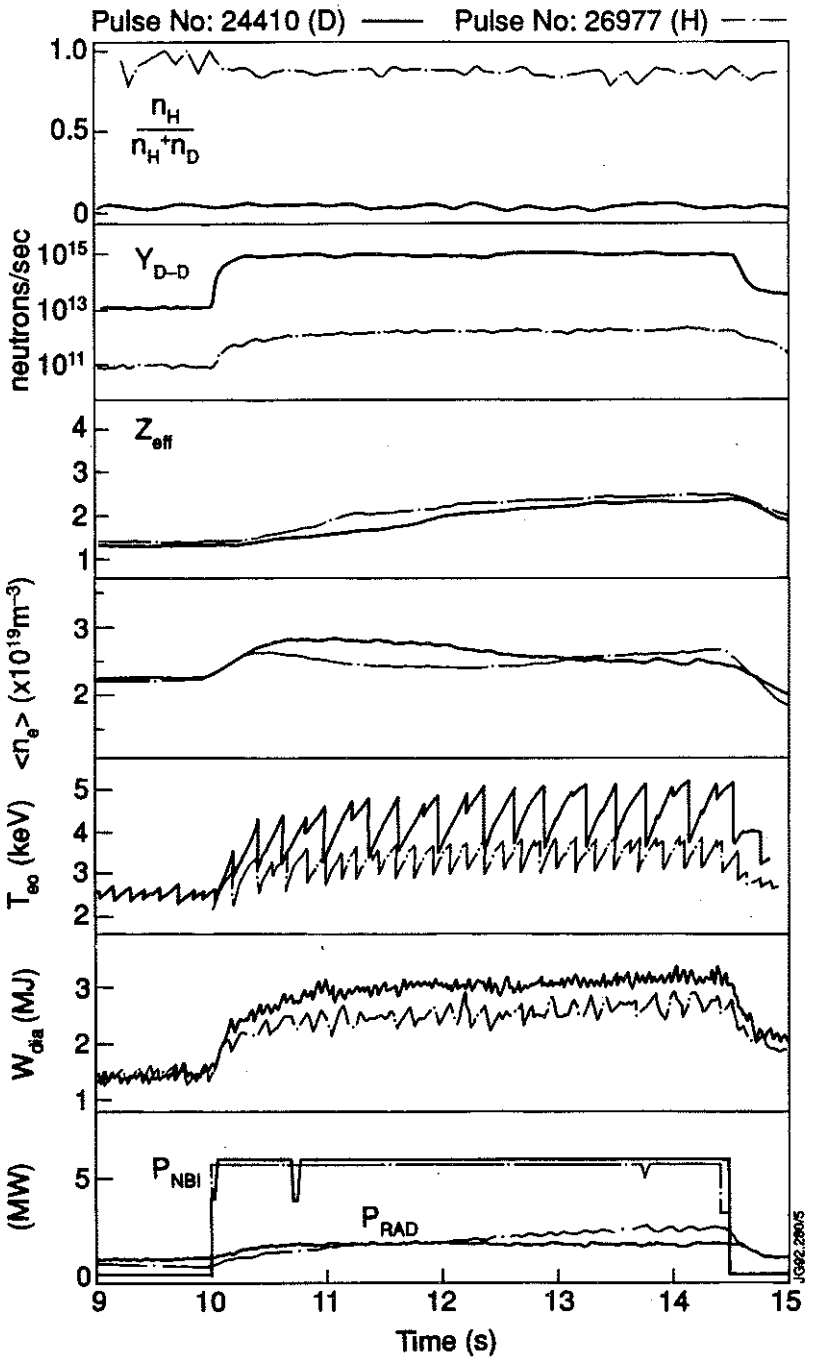

Fig. 1 Time evolution of the main plasma parameters for L-mode discharges in hydrogen and deuterium.

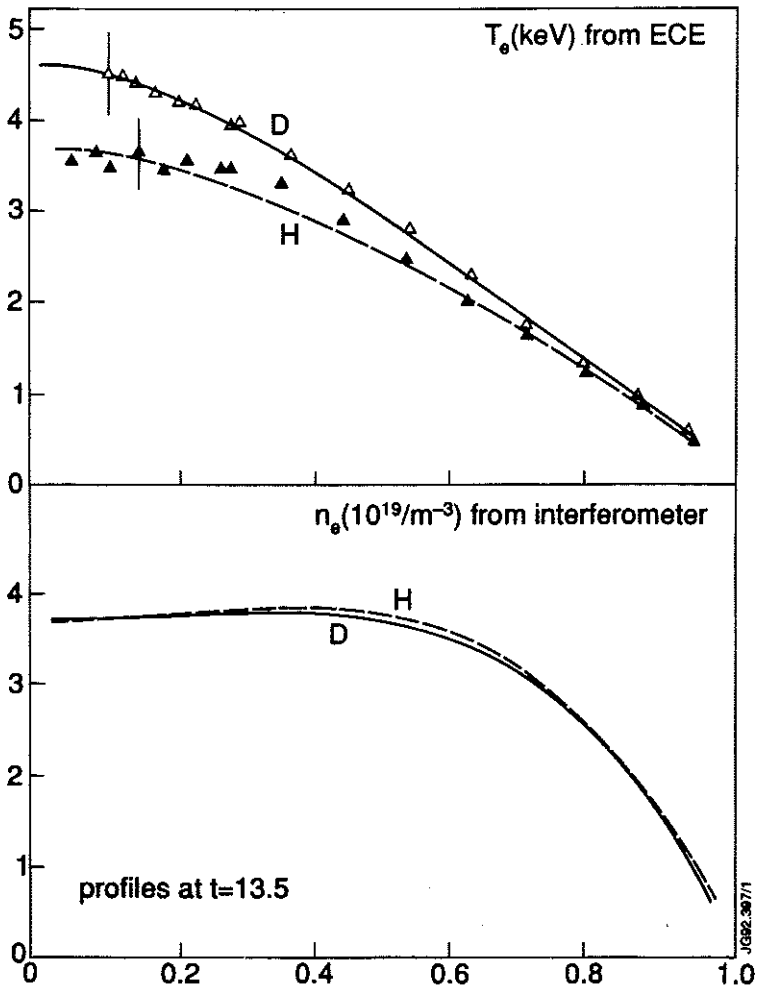

Fig. 2 Measured plasma profiles at t = 13.5 sec for the discharges in Figure 1.

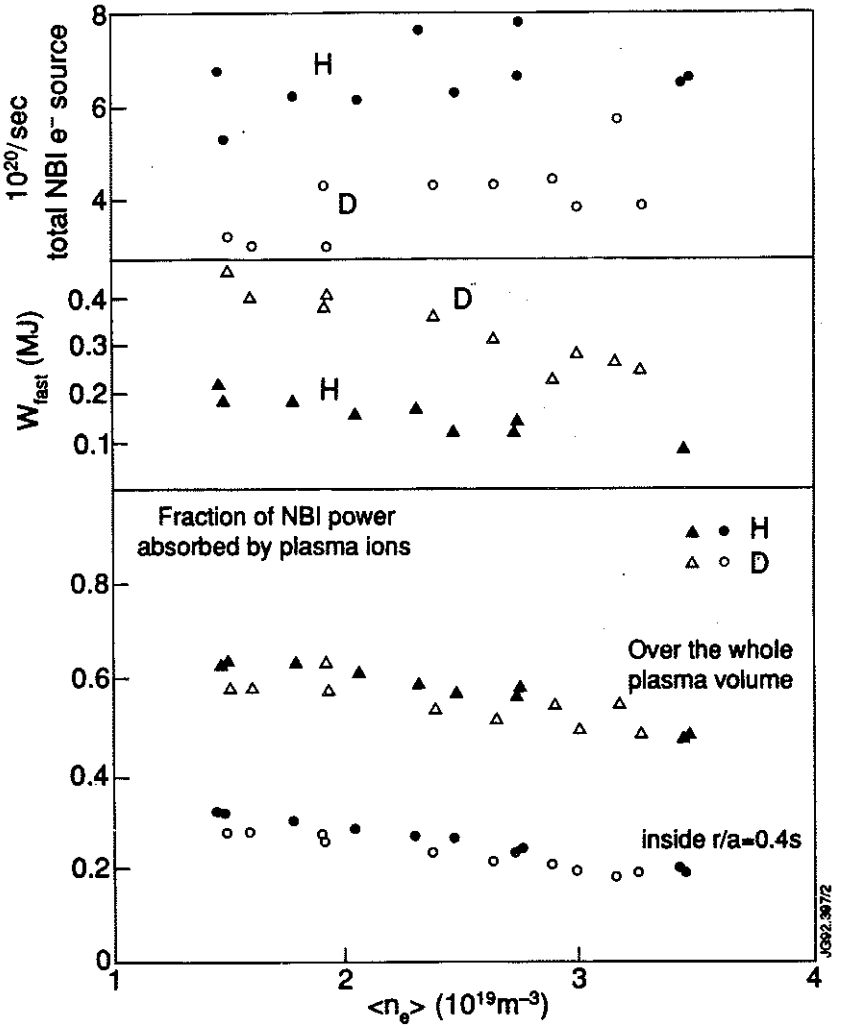

Fig. 3 Characteristics of beam-plasma interaction in hydrogen and deuterium, at different plasma densities. From top to bottom: NBI particle source, fast ion energy content and power deposition profile effects, all in steady state.

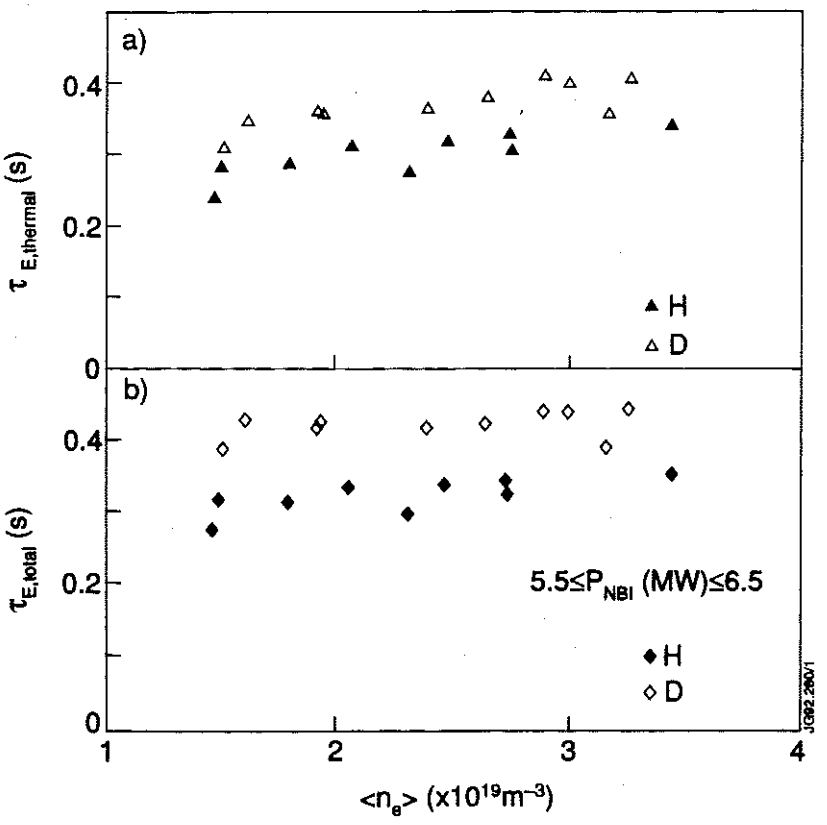

Fig. 4 Kinetic (thermal) and total (including fast ions) energy replacement time for the isotope exchange experiment.

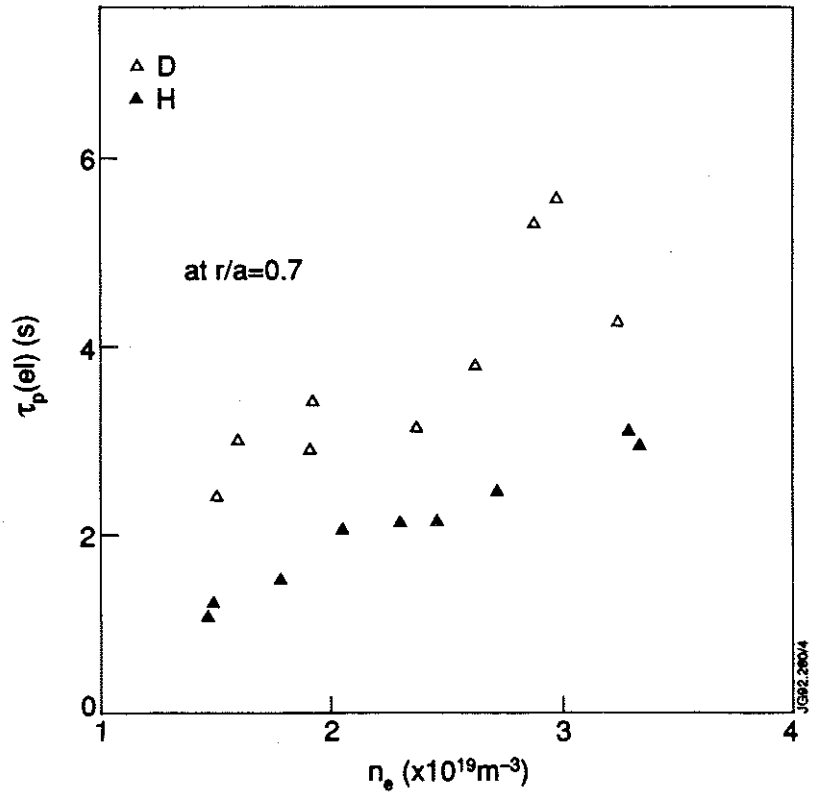

Fig. 5 Particle confinement time for the electrons in the outer region of the plasma column in hydrogen and deuterium.

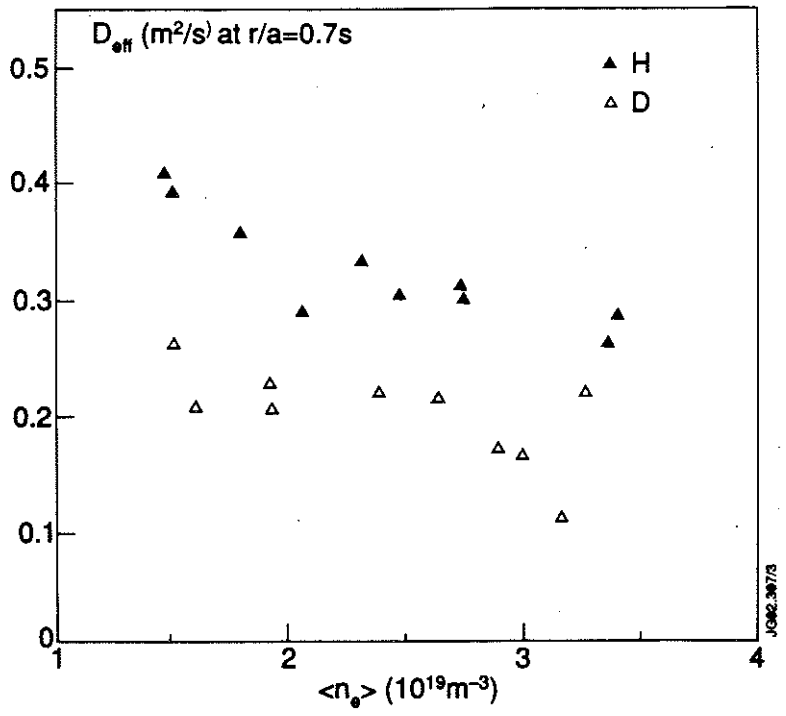

Fig. 6 Local "effective" particle diffusion coefficient (defined in the text) as a function of plasma density.

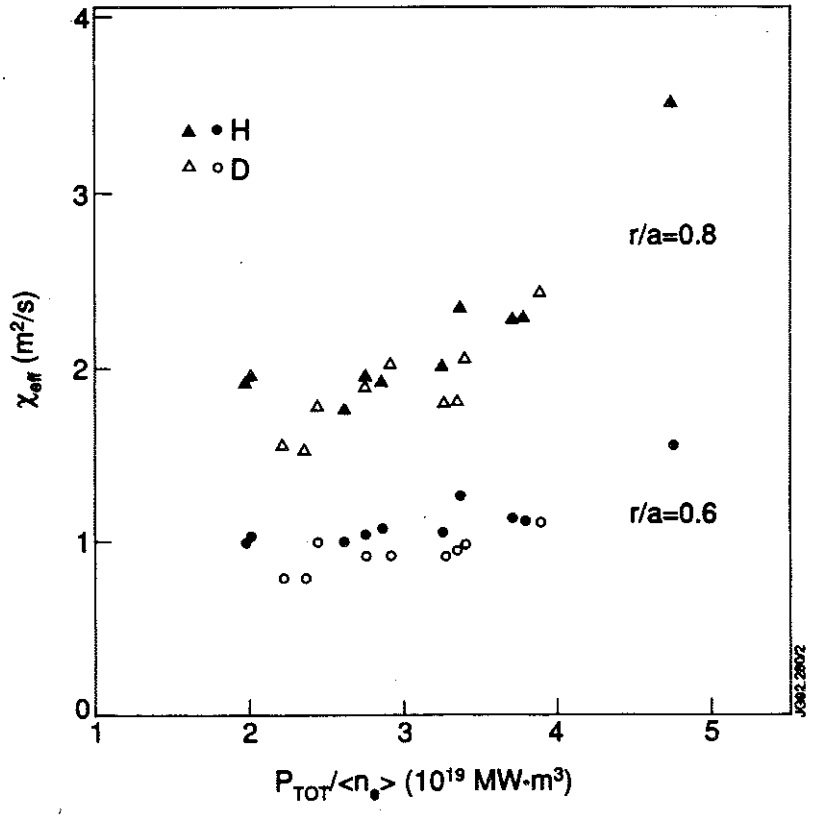

Fig. 7 Variation of the one-fluid thermal conductivity (here with $\lambda = 3/2$) with input power per particle, for H and D, at two radial locations in the plasma.

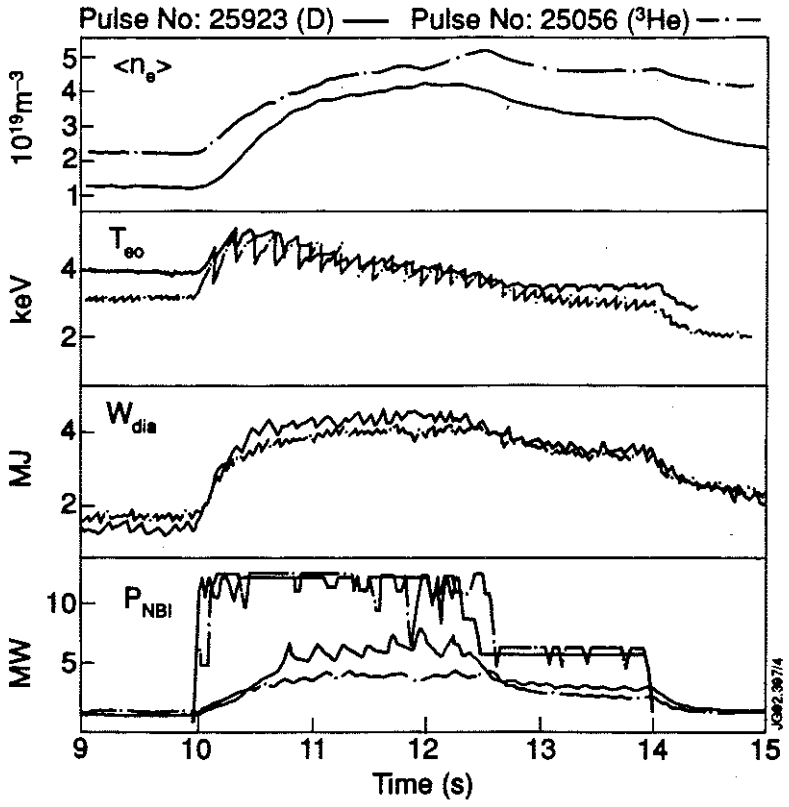

Fig. 8 Time evolution of main plasma parameters in comparable D and ^{3}He L-mode discharges.

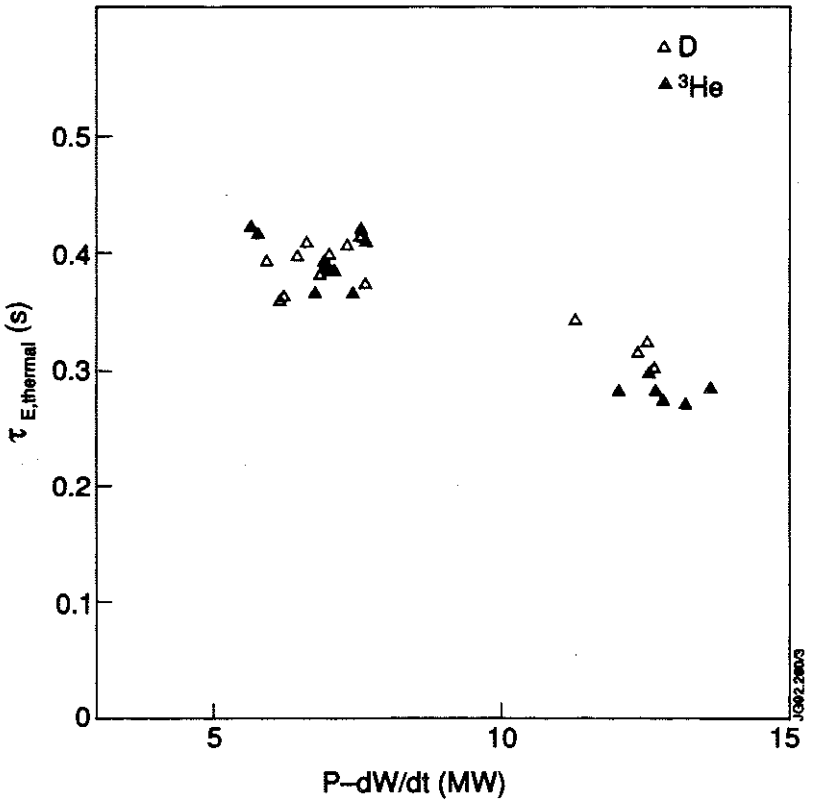

Fig. 9 Kinetic energy replacement time as a function of input power for deuterium and helium-3.

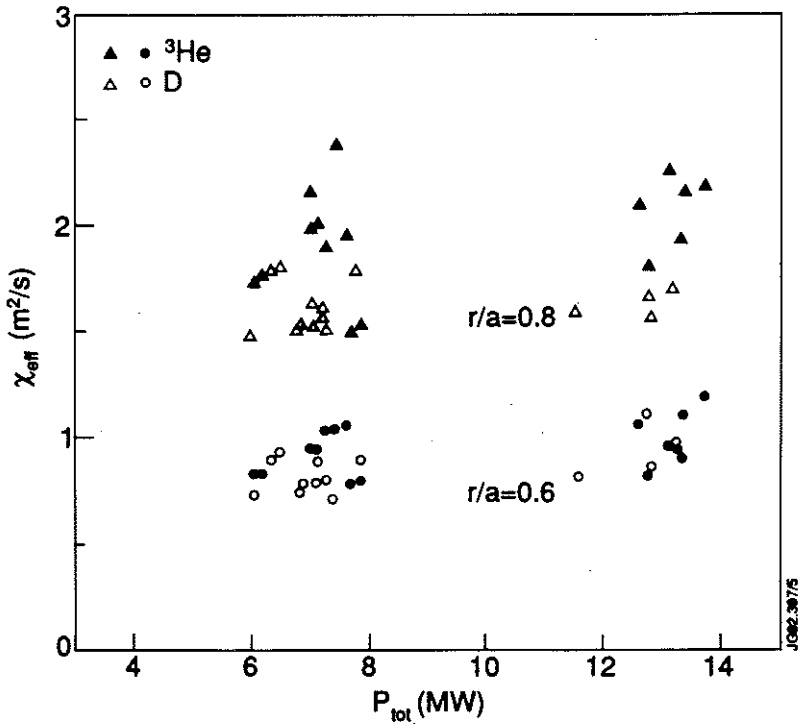

Fig. 10 One-fluid thermal conductivity vs power at two radial positions for D and ^{3}He L-modes.

Appendix I

THE JET TEAM

JET Joint Undertaking, Abingdon, Oxon, OX14 3EA, U.K.

J.M. Adams[1], B. Alper, H. Altmann, A. Andersen[14], P. Andrew, S.Ali-Arshad, W. Bailey, B. Balet, P. Barabaschi, Y. Baranov, P. Barker, R. Barnsley[2], M. Baronian, D.V. Bartlett, A.C. Bell, G. Benali, P. Bertoldi, E. Bertolini, V. Bhatnagar, A.J. Bickley, D. Bond, T. Bonicelli, S.J. Booth, G. Bosia, M. Botman, D. Boucher, P. Boucquey, M. Brandon, P. Breger, H. Brelen, W.J. Brewerton, H. Brinkschulte, T. Brown, M. Brusati, T. Budd, M. Bures, P. Burton, T. Businaro, P. Butcher, H. Buttgereit, C. Caldwell-Nichols, D.J. Campbell, D. Campling, P. Card, G. Celentano, C.D. Challis, A.V.Chankin[23], A. Cherubini, D. Chiron, J. Christiansen, P. Chuilon, R. Claesen, S. Clement, E. Clipsham, J.P. Coad, I.H. Coffey[24], A. Colton, M. Comiskey[4], S. Conroy, M. Cooke, S. Cooper, J.G. Cordey, W. Core, G. Corrigan, S. Corti, A.E. Costley, G. Cottrell, M. Cox[7], P. Crawley, O. Da Costa, N. Davies, S.J. Davies[7], H. de Blank, H. de Esch, L. de Kock, E. Deksnis, N. Deliyanakus, G.B. Denne-Hinnov, G. Deschamps, W.J. Dickson[19], K.J. Dietz, A. Dines, S.L. Dmitrenko, M. Dmitrieva[25], J. Dobbing, N. Dolgetta, S.E. Dorling, P.G. Doyle, D.F. Düchs, H. Duquenoy, A. Edwards, J. Ehrenberg, A. Ekedahl, T. Elevant[11], S.K. Erents[7], L.G. Eriksson, H. Fajemirokun[12], H. Falter, J. Freiling[15], C. Froger, P. Froissard, K. Fullard, M. Gadeberg, A. Galetsas, L. Galbiati, D. Gambier, M. Garribba, P. Gaze, R. Giannella, A. Gibson, R.D. Gill, A. Girard, A. Gondhalekar, D. Goodall[7], C. Gormezano, N.A. Gottardi, C. Gowers, B.J. Green, R. Haange, A. Haigh, C.J. Hancock, P.J. Harbour, N.C. Hawkes[7], N.P. Hawkes[1], P. Haynes[7], J.L. Hemmerich, T. Hender[7], J. Hoekzema, L. Horton, J. How, P.J. Howarth[5], M. Huart, T.P. Hughes[4], M. Huguet, F. Hurd, K. Ida[18], B. Ingram, M. Irving, J. Jacquinot, H. Jaeckel, J.F. Jaeger, G. Janeschitz, Z. Jankowicz[22], O.N. Jarvis, F. Jensen, E.M. Jones, L.P.D.F. Jones, T.T.C. Jones, J-F. Junger, F. Junique, A. Kaye, B.E. Keen, M. Keilhacker, W. Kerner, N.J. Kidd, R. Konig, A. Konstantellos, P. Kupschus, R. Lässer, J.R. Last, B. Laundy, L. Lauro-Taroni, K. Lawson[7], M. Lennholm, J.Lingertat[13], R.N. Litunovski, A. Loarte, R. Lobel, P. Lomas, M. Loughlin, C. Lowry, A.C. Maas[15], B. Macklin, C.F. Maggi[16], G. Magyar, V. Marchese, F. Marcus, J. Mart, D. Martin, E. Martin, R. Martin-Solis[8], P. Massmann, G. Matthews, H. McBryan, G. McCracken[7], P. Meriguet, P. Miele, S.F. Mills, P. Millward, E. Minardi[16], R. Mohanti[17], P.L. Mondino, A. Montvai[3], P. Morgan, H. Morsi, G. Murphy, F. Nave[27], S. Neudatchin[23], G. Newbert, M. Newman, P. Nielsen, P. Noll, W. Obert, D. O'Brien, J. O'Rourke, R. Ostrom, M. Ottaviani, S. Papastergiou, D. Pasini, B. Patel, A. Peacock, N. Peacock[7], R.J.M. Pearce, D. Pearson[12], J.F. Peng[26], R. Pepe de Silva, G. Perinic, C. Perry, M.A. Pick, J. Plancoulaine, J-P. Poffé, R. Pohlchen, F. Porcelli, L. Porte[19], R. Prentice, S. Puppin, S. Putvinskii[23], G. Radford[9], T. Raimondi, M.C. Ramos de Andrade, M. Rapisarda[29], P-H. Rebut, R. Reichle, S. Richards, E. Righi, F. Rimini, A. Rolfe, R.T. Ross, L. Rossi, R. Russ, H.C. Sack, G. Sadler, G. Saibene, J.L. Salanave, G. Sanazzaro, A. Santagiustina, R. Sartori, C. Sborchia, P. Schild, M. Schmid, G. Schmidt[6], H. Schroepf, B. Schunke, S.M. Scott, A. Sibley, R. Simonini, A.C.C. Sips, P. Smeulders, R. Smith, M. Stamp, P. Stangeby[20], D.F. Start, C.A. Steed, D. Stork, P.E. Stott, P. Stubberfield, D. Summers, H. Summers[19], L. Svensson, J.A. Tagle[21], A. Tanga, A. Taroni, C. Terella, A. Tesini, P.R. Thomas, E. Thompson, K. Thomsen, P. Trevalion, B. Tubbing, F. Tibone, H. van der Beken, G. Vlases, M. von Hellermann, T. Wade, C. Walker, D. Ward, M.L. Watkins, M.J. Watson, S. Weber[10], J. Wesson, T.J. Wijnands, J. Wilks, D. Wilson, T. Winkel, R. Wolf, D. Wong, C. Woodward, M. Wykes, I.D. Young, L. Zannelli, A. Zolfaghari[28], G. Zullo, W. Zwingmann.

PERMANENT ADDRESSES

1. UKAEA, Harwell, Didcot, Oxon, UK.
2. University of Leicester, Leicester, UK.
3. Central Research Institute for Physics, Budapest, Hungary.
4. University of Essex, Colchester, UK.
5. University of Birmingham, Birmingham, UK.
6. Princeton Plasma Physics Laboratory, New Jersey, USA.
7. UKAEA Culham Laboratory, Abingdon, Oxon, UK.
8. Universidad Complutense de Madrid, Spain.
9. Institute of Mathematics, University of Oxford, UK.
10. Freien Universität, Berlin, F.R.G.
11. Royal Institute of Technology, Stockholm, Sweden.
12. Imperial College, University of London, UK.
13. Max Planck Institut für Plasmaphysik, Garching, FRG.
14. Risø National Laboratory, Denmark.
15. FOM Instituut voor Plasmafysica, Nieuwegein, The Netherlands.
16. Dipartimento di Fisica, University of Milan, Milano, Italy.
17. North Carolina State University, Raleigh, NC, USA
18. National Institute for Fusion Science, Nagoya, Japan.
19. University of Strathclyde, 107 Rottenrow, Glasgow, UK.
20. Institute for Aerospace Studies, University of Toronto, Ontario, Canada.
21. CIEMAT, Madrid, Spain.
22. Institute for Nuclear Studies, Otwock-Swierk, Poland.
23. Kurchatov Institute of Atomic Energy, Moscow, USSR
24. Queens University, Belfast, UK.
25. Keldysh Institute of Applied Mathematics, Moscow, USSR.
26. Institute of Plasma Physics, Academica Sinica, Hefei, P. R. China.
27. LNETI, Savacem, Portugal.
28. Plasma Fusion Center, M.I.T., Boston, USA.
29. ENEA, Frascati, Italy.

At 1st July, 1992